

# Multi-stage Provincial Power Expansion Planning and Multi-market Trading Equilibrium

Guangsheng Pan, *Member, IEEE*, Zhongfan Gu, *Student Member, IEEE*, Yuanyuan Sun, *Member, IEEE*, Kaiqi Sun, *Member, IEEE*, and Wei Gu, *Senior Member, IEEE*

**Abstract**—Decarbonization in the power sector is one of the critical factors in achieving carbon neutrality, and the top-level design needs to be carried out from the perspective of power planning. A multi-stage provincial power expansion planning (PPEP) model is proposed to simulate the power expansion planning at different stages of the power systems rich in renewable energy generation. This model covers 16 types of power supply, considering macro-policy demands and micro-operation constraints. The stand-alone capacity aggregation model for coal-based units within the PPEP model allows for accurate construction and retirement with different stand-alone capacities. Moreover, the soft dynamic time warping (soft-DTW) based K-medoids technique is adopted to generate typical scenarios for balancing the model accuracy and solution efficiency. Additionally, a multi-market trading equilibrium (MMTE) mechanism is proposed to address the differences in the levelized cost of energy between the coal-based and renewable-based units by participating in energy and ancillary service markets. Since the coal-based units take on the task of providing ancillary services from renewable-based units in the ancillary service market, the MMTE mechanism can effectively equalize the profits of both by having renewable-based units purchase ancillary services from coal-based units and pay for them, thus improving the motivation of coal-based units. A case study in Xinjiang province, China, verifies the effectiveness of the planning results of the PPEP model and the profit equilibrium realization of the MMTE mechanism.

**Index Terms**—Power expansion planning, market design, ancillary service market, renewable energy generation, energy market.

## NOMENCLATURE

### A. Indices and Sets

$\Omega^{AC}, \Omega^{DC}$  Sets of AC and DC transmission lines

Manuscript received: February 16, 2024; revised: April 7, 2024; accepted: April 16, 2024. Date of CrossCheck: April 16, 2024. Date of online publication: May 3, 2024.

This work was supported in part by the National Natural Science Funds for Distinguished Young Scholar (No. 52325703), the Postdoctoral Innovation Talents Support Program (No. BX20220066), the China Postdoctoral Science Foundation (No. 2022M720709), and the Key Laboratory of Power System Intelligent Dispatch and Control of the Ministry of Education.

This article is distributed under the terms of the Creative Commons Attribution 4.0 International License (<http://creativecommons.org/licenses/by/4.0/>).

G. Pan, Z. Gu (corresponding author), and W. Gu are with the School of Electrical Engineering, Southeast University, Nanjing, China (e-mail: pgsan@163.com; gzf2206@163.com; wgu@seu.edu.cn).

Y. Sun and K. Sun are with Key Laboratory of Power System Intelligent Dispatch and Control of the Ministry of Education, School of Electrical Engineering, Shandong University, Jinan, China (e-mail: sunyy@sdu.edu.cn; skq@sdu.edu.cn).

DOI: 10.35833/MPCE.2024.000171

$\Omega^{BG}, \Omega^{CBG}$	Sets of biomass generators (BGs) and BGs with carbon capture, utilization, and storage technology (CCUS-BGs)
$\Omega^{BS}, \Omega^{PS}$	Sets of battery storage (BS) and pumped storage (PS)
$\Omega^{DC,send}, \Omega^{DC,rec}$	Sets of DC sending and DC receiving transmission lines
$\Omega^{GU}$	Set of generation units
$\Omega^{TL}$	Set of transmission lines
$\Omega^{GT}$	Set of generation units and transmission lines, $\Omega^{GT} = \Omega^{GU} \cup \Omega^{TL}$
$\Omega^{NG}, \Omega^{HG}, \Omega^{FC}$	Sets of nuclear generators (NGs), hydro generators (HGs), and fuel cells (FCs)
$\Omega^{RE}$	Set of renewable-based units
$\Omega^{TG}, \Omega^{CTG}$	Set of thermal generators (TGs) and TGs with CCUS technology (CCUS-TGs)
$d$	Index of dispatch days
$D$	Set of dispatch days
$i$	Index of generation units
$j$	Index of transmission lines
$t$	Index of dispatch hours
$T$	Set of dispatch hours
$y$	Index of year stages

### B. Functions

$COST$	Total cost of all stages
$C_y^{inv}, C_y^{mat}, C_y^{op}$	Total capital, maintenance, and operation costs at stage $y$
$C_{i,y}^{inv}, C_{i,y}^{mat}, C_{i,y}^{op}$	Capital, maintenance, and operation costs of unit $i$ at stage $y$

### C. Parameters

$\alpha_i$	Generation capacity confidence level of unit $i$
$\beta$	Generation capacity reserve ratio
$\eta_{i,y}^{wat}, \eta_{i,y}^{hyd}$	Water and hydrogen usages for per unit power of unit $i$ at stage $y$
$\sigma_j^{AC}, \sigma_j^{DC}$	AC and DC transmission losses of line $j$
$\sigma^{loss}$	Network loss
$\rho_i^{\min}, \rho_i^{\max}$	The minimum and maximum power output rates of unit $i$
$\delta_i^{rp}$	Ramping rate of unit $i$
$\xi_y$	Renewable energy penetration rate at stage $y$



$\omega_i$	Power required for per unit carbon dioxide capture of unit $i$
$\eta_i^{ccs}$	Fixed energy consumption coefficient of unit $i$
$\eta_i^{ch}, \eta_i^{dis}$	Charging and discharging efficiencies of unit $i$
$\mu_i$	The maximum capture rate of unit $i$
$\tau_{load}, \tau_{RE}$	Spinning reserve coefficients of load and renewables
$c_{i,y}^{inv}, c_{i,y}^{mat}, c_{i,y}^{op}$	Unit capital, maintenance, and operation costs of unit $i$ at stage $y$
$c_{j,y}^{inv}, c_{j,y}^{mat}, c_{j,y}^{op}$	Unit capital, maintenance, and operation cost of line $j$ at stage $y$
$c_i^{vop}, c_i^{su}, c_i^{sd}, c_i^{ccs}$	Unit variable operation, start-up, shut-down, and carbon capture costs of unit $i$
$c_y^{car}, c_y^{shed}$	Carbon tax and load shedding costs at stage $y$
$Cap_i^{max}, Cap_j^{max}$	The maximum installed capacities of unit $i$ and line $j$
$Cap_i^{sa}$	Stand-alone capacity of unit $i$
$D_{max}$	Total number of dispatch days
$e_i$	Carbon emission of unit $i$
$h_i$	Generation capacity factor of unit $i$
$H_y$	Available hydrogen amount at stage $y$
$L_{y,d,t}$	Power load at time $t$ on day $d$ at stage $y$
$L_y^{net}$	Net sending power load at stage $y$
$M$	A sufficiently large constant
$N_{i,y}, N_{j,y}$	Lifetime of unit $i$ and line $j$ at stage $y$
$p_{i,y,d,t}$	Generation capacity factor of unit $i$ at time $t$ on day $d$ at stage $y$
$r$	Discount rate
$T_{max}$	Total dispatch hours on a typical day
$T_i$	The maximum charging and discharging duration time of device $i$
$T_i^{su}, T_i^{sd}$	The minimum start-up and shut-down time of unit $i$
$W_y$	Available water amount at stage $y$

**D. Variables**

$\lambda_y^{grid}, \lambda_y^{sr}, \lambda_y^{nsr}$	Grid-connected price, spinning reserve price, and non-spinning reserve price at stage $y$
$\Delta Cap_{i,y}^{inc}, \Delta Cap_{i,y}^{dec}$	Construction and retirement capacities of unit $i$ at stage $y$
$\Delta Cap_{j,y}^{inc}, \Delta Cap_{j,y}^{dec}$	Construction and retirement capacities of line $j$ at stage $y$
$Cap_{i,y}^{total}, Cap_{j,y}^{total}$	Total installed capacities of unit $i$ and line $j$ at stage $y$
$E_{i,y,d,t}^{ccs}$	Carbon capture amount of unit $i$ at time $t$ on day $d$ at stage $y$
$LCOE_y^{COAL}, LCOE_y^{RE}$	Levelized costs of energy of coal-based and renewable-based units
$P_{i,y,d,t}$	Output power of unit $i$ at time $t$ on day $d$ at stage $y$
$P_{i,y,d,t}^{net}$	Net output power of unit $i$ at time $t$ on day $d$ at stage $y$
$P_{j,y,d,t}^{AC}$	Transmission power of AC transmission line $j$

$P_{j,y,d,t}^{DC,send}, P_{j,y,d,t}^{DC,rec}$	Sending and receiving power of DC transmission line $j$ at time $t$ on day $d$ at stage $y$
$P_{i,y,d,t}^{ch}, P_{i,y,d,t}^{dis}$	Charging and discharging power of unit $i$ at time $t$ on day $d$ at stage $y$
$P_{i,y,d,t}^{on}, P_{i,y,d,t}^{su}, P_{i,y,d,t}^{sd}, P_{i,y,d,t}^{shed}$	Online, start-up, and shut-down capacities of unit $i$ at time $t$ on day $d$ at stage $y$
$P_{i,y,d,t}^{sr}, P_{j,y,d,t}^{sr}$	Spinning reserve of unit $i$ and line $j$ at time $t$ on day $d$ at stage $y$
$REV_y^{RE}, REV_y^{COAL}, REV_y^{RE,ELE}, REV_y^{COAL,ELE}, REV_y^{COAL,sr}, REV_y^{COAL,nsr}$	Net revenues of renewable-based and coal-based units at stage $y$ Electricity sales revenue of renewable-based and coal-based units at stage $y$ Revenue from spinning and non-spinning reserves provided by coal-based to renewable-based units at stage $y$
$S_{i,y,d,t}$	Storage capacity of device $i$ at time $t$ on day $d$ at stage $y$

I. INTRODUCTION

CARBON neutrality is gradually becoming a global consensus, and energy transition is imminent [1]. As one of the crucial sources of carbon emissions, it is necessary to realize carbon neutrality in the power sector in advance, and therefore, building power systems rich in renewable energy generation has become a common goal for most countries [2]. However, the process is lengthy and requires addressing critical challenges.

The first and foremost challenge is power planning [3], [4]. Accurately and efficiently predicting the power mix at each stage is a major policy challenge, especially with regard to the construction and retirement of coal-based units.

The second key challenge is motivating generation units. Cheap electricity from renewable-based units and carbon emission policy restrictions are leading to the large-scale retirement of coal-based units [5]. The remaining coal-based units assume the peaking function but at a much higher cost than renewable-based units. Incentivizing the profit-oriented generators of coal-based units becomes another challenge.

Several scholars have conducted studies to tackle the challenges in power system planning around the world [3], [6]-[14]. Reference [8] investigated the effectiveness of five complementary approaches for intermittent renewable energy integration at the most economical rate in 2050 in Western Europe, but it only considered a single year without integrating multiple years for an overall assessment. Reference [9] integrated a prospective life cycle assessment with a comprehensive global model encompassing energy, economy, land use, and climate, aiming to investigate the life-cycle emissions of an envisioned low-carbon power system and its implications on selecting technologies. However, the broad scope of the study leads to less comprehensive modeling considerations. Reference [10] formulated an integrated model for gas and power network planning to scrutinize the influ-

ence of different emission strategies on the gas network expansion of the UK in the 2050s. The study focuses on the gas network and is not comprehensive in considering and modeling the power network. It also only considers planning for a single year. Considering the limitations of a single year, [11] integrated long-duration energy system with high-resolution power system modeling based on multi-year data to achieve power system planning for the UK in 2050. Although the study fully utilized multi-year data, it could only obtain planning results for the target years and not for the transition years. Additionally, as one of the largest countries in terms of carbon emissions, many scholars have conducted extensive research focusing on China. One such study [3] evaluated the power planning and power generation costs at 75% renewable energy penetration by 2035 using the annual time-series technique in Northwest China. However, this study had limitations, considering only 5 types of power supply and single-stage planning. In 2020, a multi-stage planning model called the SwitchChina model was proposed in [12], which examined power supply planning over 3 stages from 2015 to 2030, fully considering spinning and non-spinning reserve constraints and extending the types of power supply to 11. However, the resolution of the SwitchChina model was about 6 hours, neglecting important output characteristics of renewable-based units and not considering the possibility of applying carbon capture, utilization, and storage (CCUS) technologies. Drawing from [3], a detailed model was introduced, demonstrating the viability and cost competitiveness of achieving carbon neutrality by 2050 [13]. Nevertheless, the planning horizon of this model was limited to a single stage and overlooked the potential of CCUS technologies and fuel cells. In response, [14] presented a multi-stage expansion model of generation and transmission at the provincial level, incorporating various power sources and ensuring sufficient reserve constraints. However, this model did not consider the variation of equipment parameters over the planning horizon or the promising technology such as fuel cells.

In summary, current research has yet to fully address the challenge of achieving a harmonious equilibrium between model intricacy and accuracy of solutions. It is exacerbated by the inadequate attention paid to power supply options, specifically the potential of hydrogen-based units. In modeling, there is a pressing need to conduct more in-depth studies on high-resolution modeling and scenario generation technology. Additionally, a dearth of works on the refined modeling involved in retiring and constructing coal-based units, which plays a pivotal role in energy transition.

Recent research in market mechanism design has explored various markets, including the energy market [15]-[18], the ancillary service market [19]-[22], and the emerging inertia market [23]-[26]. Studies have shown that centralized energy markets and ancillary service markets are well-established, with energy and ancillary services often traded through competitive bidding [27]. Decentralized market mechanisms, such as peer-to-peer (P2P) energy trading markets, have also been extensively studied. One example is the P2P transactive energy model for multi-microgrids developed by [17], which

guarantees the security of power distribution network and allows multi-microgrids to trade energy with each other flexibly. In addition, an energy trading framework by combining blockchain and distributed optimization was proposed to prevent energy market failures caused by dishonest participants [18]. Some scholars have even created a P2P joint energy and reserve market mechanism to streamline clearing energy and reserve markets [21]. Moreover, a performance ratio has been suggested to quantify the response rate [22], which is integrated into the real-time market-clearing process to enhance the primary frequency response service. The inertia market has been exciting to scholars due to its significant role in accommodating renewable energy. Reference [23] proposed a product that ensures non-negative returns based on the Vickrey-Clarke-Groves payment rule to compensate virtual inertia agents [23]. However, this rule is complex and challenging to apply in practice. Reference [24] proposed a chance-constrained stochastic unit commitment model that incorporated inertia requirements to price inertial services and demonstrated its effectiveness. In another study, an investment equilibrium model was developed based on the Stackelberg game theory that considered the inertia, energy, standby, and capacity markets [25]. Furthermore, there are ongoing efforts to combine inertia, primary frequency response, and the design of energy market mechanisms [26].

Numerous scholars have delved deeply into the study of centralized and decentralized energy markets and ancillary service markets. Lately, there has been a growing interest in inertial markets. Nevertheless, it significantly challenges harmonizing the market mechanisms with the energy structure as it shifts from coal-based power to renewable-based power. Therefore, it is crucial to design market mechanisms that cater to the specific equilibrium of interests between coal-based and renewable-based units.

To fill the research gaps identified above, this paper proposes a multi-stage provincial power expansion planning (PPEP) model to predict the future power structure. A multi-market trading equilibrium (MMTE) mechanism is further proposed for the equilibrium of interests between coal-based and renewable-based units. The contributions of this paper are summarized as follows.

- 1) A comprehensive multi-stage PPEP model is proposed, covering 16 types of power supply, 5 kinds of macro-policy demands, and 12 kinds of micro-operation constraints.

- 2) The soft dynamic time warping (soft-DTW) based  $K$ -medoids technique is adopted to accelerate the model solution, and the stand-alone capacity aggregation model of coal-based units is embedded in the PPEP model to accurately characterize the construction and retirement processes.

- 3) To eliminate the lack of economics of coal-based units participating in peak regulation in the future, the MMTE mechanism is proposed for the equilibrium of interests between coal-based and renewable-based units.

The remainder of this paper is organized as follows. Section II introduces the research framework. Section III presents the modeling of the PPEP model. Section IV designs the MMTE mechanism. Section V presents the analysis of case studies. The conclusions are presented in Section VI.

## II. RESEARCH FRAMEWORK

This section presents a comprehensive research framework comprising two main parts, as depicted in Fig. 1. The first part focuses on formulation process of PPEP model, while the second part delves into the design of MMTE mechanism. To comprehensively consider the role of all types of power supply in the energy transition, we formulate the

PPEP model that encompasses 16 types of power supply including generation units and transmission lines, as given in Table I. The PPEP model considers macro-policy demands and micro-operational constraints and accurately simulates the retirement and construction of coal-based units at each stage. In Fig. 1,  $c$ ,  $b$ ,  $f$ , and  $g$  are the coefficient vectors;  $A$ ,  $D$ ,  $E$ , and  $G$  are the coefficient matrices; and  $x$  and  $y$  are the decision variables.

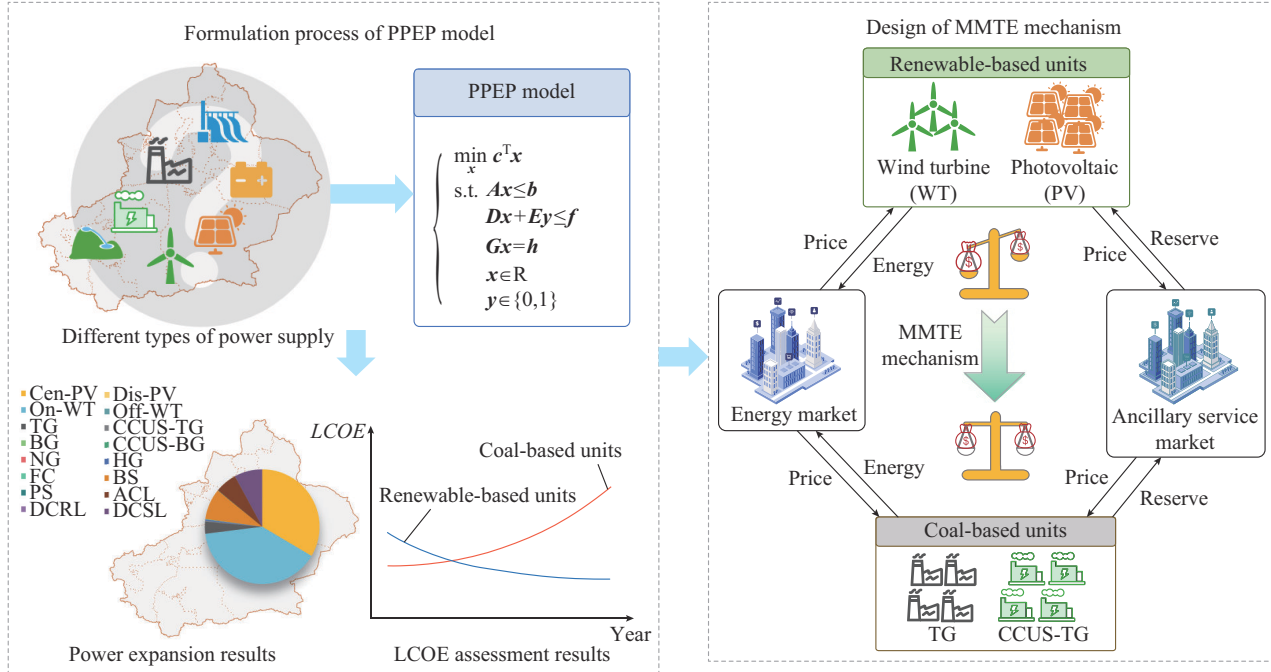


Fig. 1. Research framework.

TABLE I  
LIST OF 16 TYPES OF POWER SUPPLY

No.	Type	No.	Type
1	Centralized PV (Cen-PV)	9	Fuel cell (FC)
2	Distributed PV (Dis-PV)	10	Battery storage (BS)
3	Offshore WT (Off-WT)	11	Pumped storage (PS)
4	Onshore WT (On-WT)	12	Nuclear generator (NG)
5	Thermal generator (TG)	13	Hydro generator (HG)
6	Biomass generator (BG)	14	AC transmission line (ACL)
7	TG with CCUS technology (CCUS-TG)	15	DC receiving transmission line (DCRL)
8	BG with CCUS technology (CCUS-BG)	16	DC sending transmission line (DCSL)

Based on the results of the PPEP model, we can establish the functional positioning of coal-based and renewable-based units at different stages. Predictably, the levelized cost of energy (LCOE) of coal-based units will increase over time due to carbon emission policies, while the LCOE of renewable-based units will decrease, reducing the incentive of coal-based units for power generation.

Offering economic subsidies from a market perspective is necessary and adequate to encourage coal-based units. The MMTE mechanism is proposed to ensure an equilibrium of interests between the coal-based and renewable-based units.

In addition to selling electricity in the energy market, the coal-based units take on the additional task of providing ancillary services for the renewable-based units. The renewable-based units compensate the coal-based units by purchasing these ancillary services, and a fair equilibrium between the two can be achieved through reasonable market trading.

## III. MODELING OF PPEP MODEL

The PPEP model needs to meet two sets of constraints: ① macro-level planning constraints, which describe equipment expansion and environmental policy considerations at the planning stage; and ② micro-level operation constraints, which model power balance and generation characteristics of the generation units during operation.

### A. Macro-level Planning Constraints

#### 1) The Maximum Development Potential Constraints of Renewable-based Units

Formula (1) ensures that the total installed capacity of renewable-based units does not exceed their maximum exploitable configuration potential.

$$0 \leq Cap_{i,y}^{total} \leq Cap_i^{max} \quad \forall i \in \Omega^{RE}, y \in [1, 8] \quad (1)$$

#### 2) Installed Capacity Continuity Constraints for Generation Units

Formula (2) models the expansion and retirement capacity

changes of generation units. Furthermore, (3) and (4) limit the expansion and retirement rates of generation units, respectively, where  $5/N_{i,y}$  is the natural retirement rate of generation units at each stage [14]. It is worth noting that (5) ensures that the capacity of transmission lines and CCUS-TGs at each stage is equal to that at the initial stage, which means that the retirement of transmission lines and CCUS-TG is not considered.

$$Cap_{i,y}^{total} = Cap_{i,y-1}^{total} + \Delta Cap_{i,y}^{inc} - \Delta Cap_{i,y}^{dec} \quad \forall i \in \Omega^{GT}, y \in [1, 8] \quad (2)$$

$$0 \leq \Delta Cap_{i,y}^{inc} \quad \forall i \in \Omega^{GT}, y \in [1, 8] \quad (3)$$

$$(5/N_{i,y}) \cdot Cap_{i,y-1}^{total} \leq \Delta Cap_{i,y}^{dec} \leq Cap_{i,y-1}^{total} \quad \forall i \in \Omega^{GU} \setminus \Omega^{CTG}, y \in [1, 8] \quad (4)$$

$$\Delta Cap_{i,y}^{dec} = \Delta Cap_{j,y}^{dec} = 0 \quad \forall i \in \Omega^{CTG}, j \in \Omega^{TL}, y \in [1, 8] \quad (5)$$

In particular, a refined model is developed to simulate the construction and retirement of TGs depending on their stand-alone capacity. Therefore, their installed capacity is additionally constrained by (6)-(9) to ensure that the construction and retirement capacity of TGs is not smaller than their stand-alone capacity or no TGs are constructed/retired at each stage.

$$-M(1 - \varepsilon_{i,y}^{inc}) \leq \Delta Cap_{i,y}^{inc} \leq M(1 - \varepsilon_{i,y}^{inc}) \quad \forall i \in \{\Omega^{TG}, \Omega^{CTG}\}, y \in [1, 8] \quad (6)$$

$$-M(1 - \varepsilon_{i,y}^{dec}) \leq \Delta Cap_{i,y}^{dec} \leq M(1 - \varepsilon_{i,y}^{dec}) \quad \forall i \in \Omega^{TG}, y \in [1, 8] \quad (7)$$

$$Cap_i^{sa} - \Delta Cap_{i,y}^{inc} \leq M\varepsilon_{i,y}^{inc} \quad \forall i \in \{\Omega^{TG}, \Omega^{CTG}\}, y \in [1, 8] \quad (8)$$

$$Cap_i^{sa} - \Delta Cap_{i,y}^{dec} \leq M\varepsilon_{i,y}^{dec} \quad \forall i \in \Omega^{TG}, y \in [1, 8] \quad (9)$$

where the binary variables  $\varepsilon_{i,y}^{inc}$  and  $\varepsilon_{i,y}^{dec}$  equal 1 when TGs are not constructed/retired; otherwise they equal 0.

### 3) Water and Hydrogen Consumption Constraints

At the planning stage, the natural water resource of the region limits the installed capacity of the power source, which has been taken into account in [14]. Here, in addition to water consumption constraints, hydrogen consumption constraints are added because power generation from hydrogen will represent only 5%-10% of the local hydrogen demand in the future [28]. The consumption of raw materials for generation unit is not negligible, and (10) and (11) give the limits for the total water consumption by the generation units and hydrogen consumption by the FC subject to provincial regions, respectively.

$$\frac{8760}{D_{\max} T_{\max}} \sum_{i \in \Omega^{GU} \setminus \{\Omega^{BS}, \Omega^{PS}\}} \sum_{d \in D} \sum_{t \in T} \eta_{i,y}^{wat} P_{i,y,d,t} \leq W_y \quad \forall y \in [1, 8] \quad (10)$$

$$\frac{8760}{D_{\max} T_{\max}} \sum_{i \in \Omega^{FC}} \sum_{d \in D} \sum_{t \in T} \eta_{i,y}^{hyd} P_{i,y,d,t} \leq H_y \quad \forall y \in [1, 8] \quad (11)$$

where  $8760/(D_{\max} T_{\max})$  is intended to discount the consumption amount of typical days to the cost of each stage.

### 4) Renewable Energy Penetration Constraints

China seeks to achieve carbon peaking by 2030 and carbon neutrality by 2060. Reference [29] projected China's energy mix between 2030 and 2060. Based on the projections, we calculate renewable energy penetration rates at each stage to constrain the proportion of renewable energy generation, as shown in (12).

$$\sum_{i \in \Omega^{RE}} \sum_{d \in D} \sum_{t \in T} P_{i,y,d,t} \geq \zeta_y \left( \sum_{i \in \Omega^{GU} \setminus \{\Omega^{CTG}, \Omega^{CBG}, \Omega^{BS}, \Omega^{PS}\}} \sum_{d \in D} \sum_{t \in T} P_{i,y,d,t} + \sum_{i \in \{\Omega^{CTG}, \Omega^{CBG}\}} \sum_{d \in D} \sum_{t \in T} P_{i,y,d,t}^{net} \right) \quad \forall y \in [1, 8] \quad (12)$$

### 5) Capacity Reserve Constraints

Uncertainties in source-side renewable energy generation and load-side power load significantly impact the planning results, and it is necessary to consider them accordingly at the planning stage. Here, we use the generation capacity confidence level to characterize the generation uncertainty of different types of generation units and the generation capacity reserve ratio to characterize the load uncertainty, as shown in (13). It means that the sum of the capacities of all generation units in the region and the input capacity of the DC transmission line must be greater than the peak local power load and the output load of the DC transmission line with some margin. Note that it is merely a response to the source-load uncertainty from the capacity planning stage to make the planning result robust. The spinning reserve constraints at the operation stage will ensure that the system can cope with contingencies.

$$\sum_{i \in \Omega^{GU}} \alpha_i \cdot Cap_{i,y}^{total} + \sum_{j \in \Omega^{DC,rec}} Cap_{j,y}^{total} \geq (1 + \beta) \left( \max_{d \in D, t \in T} L_{y,d,t} + \sum_{j \in \Omega^{DC,send}} Cap_{j,y}^{total} \right) \quad \forall y \in [1, 8] \quad (13)$$

It should be noted that, for the DC transmission line, the sending end is supplied with delivered power by dedicated units, and the receiving end serves as dispatchable units so that the DC transmission line enables the transmission of reserve power in this model. In contrast, according to the area control error, the ACL determines the direction of power delivery. Thus, there are no defined receiving and sending ends, and the possibility of the ACL participating in the reserve is not considered in the PPEP model [14].

### B. Micro-level Operation Constraints

#### 1) Constraints of Provincial Power Balance

In the PPEP model, we consider hourly power balance, as shown in (14).

$$\sum_{i \in \Omega^{GU} \setminus \{\Omega^{CTG}, \Omega^{CBG}, \Omega^{BS}, \Omega^{PS}\}} P_{i,y,d,t} + \sum_{i \in \{\Omega^{CTG}, \Omega^{CBG}\}} P_{i,y,d,t}^{net} + \sum_{j \in \Omega^{AC}} P_{j,y,d,t}^{AC} + \sum_{i \in \{\Omega^{BS}, \Omega^{PS}\}} (P_{i,y,d,t}^{dis} - P_{i,y,d,t}^{ch}) - \sum_{j \in \Omega^{DC,send}} P_{j,y,d,t}^{DC,send} + \sum_{j \in \Omega^{DC,rec}} (1 - \sigma_j^{DC}) P_{j,y,d,t}^{DC,rec} = \frac{L_{y,d,t} - P_{y,d,t}^{shed}}{1 - \sigma_{loss}} \quad \forall y \in [1, 8], d \in D, t \in T \quad (14)$$

#### 2) Constraints of Provincial Net Transmission Power Balance

The annual net receiving or sending power for a provincial region should meet the actual operation, as shown in (15).

$$\frac{8760}{D_{\max} T_{\max}} \left[ \sum_{j \in \Omega^{DC,send}} \sum_{d \in D} \sum_{t \in T} P_{j,y,d,t}^{DC,send} - \sum_{j \in \Omega^{DC,rec}} \sum_{d \in D} \sum_{t \in T} (1 - \sigma_j^{DC}) P_{j,y,d,t}^{DC,rec} - \sum_{j \in \Omega^{AC}} \sum_{d \in D} \sum_{t \in T} P_{j,y,d,t}^{AC} \right] = \frac{L_y^{net}}{1 - \sigma_{loss}} \quad \forall y \in [1, 8] \quad (15)$$

### 3) Constraints of Load Shedding

Further, the load shedding power of a region should not exceed its power load, as shown in (16).

$$0 \leq P_{y,d,t}^{shed} \leq L_{y,d,t} \quad \forall y \in [1, 8], d \in D, t \in T \quad (16)$$

### 4) Constraints of Transmission Line

Considering that the PPEP model is oriented to provincial regions, we reasonably regard provincial regions as nodes of transmission lines, which can effectively avoid introducing complex power flow forms. On this basis, the power transmitted by AC and DC transmission lines can be freely dispatched within the transmission capacity limits, avoiding the introduction of binary variables. In fact, this assumption has been widely used in grid planning at the national or provincial level [12], [13], when line losses will be proportional to the transmitted power.

Formulas (17)-(20) present the model of ACLs.  $P_{j,y,d,t}^{AC,rec}$  and  $P_{j,y,d,t}^{AC,send}$  are auxiliary variables to model the line loss of ACL. The ACL has a bi-directional power flow, but the transmission direction is unique at one moment. In order to facilitate the modeling of line losses, the power flow direction at one moment is decoupled into the incoming and outgoing power flows by introducing auxiliary variables in the form of this model.

$$P_{j,y,d,t}^{AC} = (1 - \sigma_j^{AC}) P_{j,y,d,t}^{AC,rec} - P_{j,y,d,t}^{AC,send} \quad \forall j \in \Omega^{AC}, y \in [1, 8], d \in D, t \in T \quad (17)$$

$$0 \leq P_{j,y,d,t}^{AC,send} \leq Cap_{j,y}^{total} \quad \forall j \in \Omega^{AC}, y \in [1, 8], d \in D, t \in T \quad (18)$$

$$0 \leq P_{j,y,d,t}^{AC,rec} \leq Cap_{j,y}^{total} \quad \forall j \in \Omega^{AC}, y \in [1, 8], d \in D, t \in T \quad (19)$$

$$-Cap_{j,y}^{total} \leq P_{j,y,d,t}^{AC} \leq Cap_{j,y}^{total} \quad \forall j \in \Omega^{AC}, y \in [1, 8], d \in D, t \in T \quad (20)$$

Formulas (21) and (22) are for DC transmission lines, which differ from ACLs in that DC transmission lines allow only unidirectional power flow.

$$0 \leq P_{j,y,d,t}^{DC,send} \leq Cap_{j,y}^{total} \quad \forall j \in \Omega^{DC,send}, y \in [1, 8], d \in D, t \in T \quad (21)$$

$$0 \leq P_{j,y,d,t}^{DC,rec} \leq Cap_{j,y}^{total} \quad \forall j \in \Omega^{DC,rec}, y \in [1, 8], d \in D, t \in T \quad (22)$$

### 5) Operation Constraints of TGs

Considering that the TGs are important participants in the peak and frequency regulation of the power system, it is necessary to model their operation states accurately. When simulating the operation of TGs, we use continuous variables to characterize their start-up/shut-down states [13], which avoids the introduction of binary variables and can effectively improve the speed of model solution. Formula (23) provides the lower limit on the capacity of TGs, (24) simulates the variation of hourly on-line capacity, with upper and lower limits constrained by (25) and (26), respectively, to ensure that the start-up and shut-down of TGs satisfy the minimum time. Formula (27) limits the output power range of the units, and (28) is used to characterize the ramping characteristics of TGs.

$$\begin{cases} 0 \leq P_{i,y,d,t}^{on} \\ 0 \leq P_{i,y,d,t}^{su} \\ 0 \leq P_{i,y,d,t}^{sd} \end{cases} \quad \forall i \in \{\Omega^{TG}, \Omega^{CTG}\}, y \in [1, 8], d \in D, t \in T \quad (23)$$

$$P_{i,y,d,t}^{on} = P_{i,y,d,t-1}^{on} + P_{i,y,d,t}^{su} - P_{i,y,d,t}^{sd} \quad \forall i \in \{\Omega^{TG}, \Omega^{CTG}\}, y \in [1, 8], d \in D, t \in T \quad (24)$$

$$P_{i,y,d,t}^{on} \geq \sum_{\tau=0}^{T_i^{su}} P_{i,y,d,t-\tau}^{su} \quad t > T_i^{su}, \forall i \in \{\Omega^{TG}, \Omega^{CTG}\}, y \in [1, 8], d \in D, t \in T \quad (25)$$

$$P_{i,y,d,t}^{on} \leq Cap_{i,y}^{total} - \sum_{\tau=0}^{T_i^{sd}} P_{i,y,d,t-\tau}^{sd} \quad t > T_i^{sd}, \forall i \in \{\Omega^{TG}, \Omega^{CTG}\}, y \in [1, 8], d \in D, t \in T \quad (26)$$

$$\rho_i^{\min} P_{i,y,d,t}^{on} \leq P_{i,y,d,t} \leq \rho_i^{\max} P_{i,y,d,t}^{on} \quad \forall i \in \{\Omega^{TG}, \Omega^{CTG}\}, y \in [1, 8], d \in D, t \in T \quad (27)$$

$$-\delta_i^{rp} P_{i,y,d,t}^{on} \leq P_{i,y,d,t} - P_{i,y,d,t-1} \leq \delta_i^{rp} P_{i,y,d,t}^{on} \quad \forall i \in \{\Omega^{TG}, \Omega^{CTG}\}, y \in [1, 8], d \in D, t \in T \quad (28)$$

### 6) Operation Constraints of BGs and HGs

Since BGs and HGs are not easy to control compared with TGs and their capacity to participate in power system operation is limited, the aggregation models are widely used in their operation, as shown in (29) and (30).

$$\rho_i^{\min} \cdot Cap_{i,y}^{total} \leq P_{i,y,d,t} \leq Cap_{i,y}^{total} \quad \forall i \in \{\Omega^{BG}, \Omega^{CBG}, \Omega^{HG}\}, y \in [1, 8], d \in D, t \in T \quad (29)$$

$$\sum_{d \in D} \sum_{t \in T} P_{i,y,d,t} \leq \frac{D_{\max} T_{\max} h_i}{8760} \cdot Cap_{i,y}^{total} \quad \forall i \in \{\Omega^{BG}, \Omega^{CBG}, \Omega^{HG}\}, y \in [1, 8] \quad (30)$$

### 7) Operation Constraints of NGs

Like TGs, the output power of NGs is also modeled by continuous variables, as shown in (31)-(34). Considering the inflexibility of start-up and shut-down of NGs, (35) further constrains the output power of NGs to remain constant during one day.

$$\begin{cases} 0 \leq P_{i,y,d,t}^{on} \leq Cap_{i,y}^{total} \\ 0 \leq P_{i,y,d,t}^{su} \leq Cap_{i,y}^{total} \\ 0 \leq P_{i,y,d,t}^{sd} \leq Cap_{i,y}^{total} \end{cases} \quad i \in \Omega^{NG}, y \in [1, 8], d \in D, t \in T \quad (31)$$

$$P_{i,y,d,0}^{on} = P_{i,y,d-1,T_{\max}}^{on} + P_{i,y,d-1,T_{\max}}^{su} - P_{i,y,d-1,T_{\max}}^{sd} \quad \forall i \in \Omega^{NG}, y \in [1, 8], d \in D \quad (32)$$

$$\rho_i^{\min} P_{i,y,d,t}^{on} \leq P_{i,y,d,t} \leq P_{i,y,d,t}^{on} \quad \forall i \in \Omega^{NG}, y \in [1, 8], d \in D, t \in T \quad (33)$$

$$\sum_{d \in D} \sum_{t \in T} P_{i,y,d,t} \leq \frac{D_{\max} T_{\max} h_i}{8760} \cdot Cap_{i,y}^{total} \quad \forall i \in \Omega^{NG}, y \in [1, 8] \quad (34)$$

$$P_{i,y,d,t} = P_{i,y,d,t-1} \quad \forall i \in \Omega^{NG}, y \in [1, 8], d \in D, t \in T \quad (35)$$

### 8) Operation Constraints of CCUS-TG and CCUS-BG

Generation units with CCUS technology can effectively capture carbon but they are expensive, and the capture process will consume more power, so the net output of a generation unit with CCUS technology will be smaller than that of a generation unit without CCUS. The net output of CCUS-TG and CCUS-BG is shown in (36) and limited by (37). Further, CCUS-TG and CCUS-BG can change the net output and carbon emissions by adjusting the intensity of carbon capture, which is modeled by (38). In addition, the operation of CCUS-TG and CCUS-BG is still subject to (23)-(30) of conventional TGs and BGs, which are not repeated here.

$$P_{i,y,d,t}^{net} = P_{i,y,d,t} - \omega_i E_{i,y,d,t}^{ccs} - \eta_i^{ccs} \cdot Cap_{i,y}^{total} \quad \forall i \in \{\Omega^{CTG}, \Omega^{CBG}\}, y \in [1, 8], d \in D, t \in T \quad (36)$$

$$0 \leq P_{i,y,d,t}^{net} \quad \forall i \in \{\Omega^{CTG}, \Omega^{CBG}\}, y \in [1, 8], d \in D, t \in T \quad (37)$$

$$0 \leq E_{i,y,d,t}^{ccs} \leq \mu_i e_i P_{i,y,d,t} \quad \forall i \in \{\Omega^{CTG}, \Omega^{CBG}\}, y \in [1, 8], d \in D, t \in T \quad (38)$$

### 9) Operation Constraints of Variable Renewable-based Units

For intermittent renewable-based units such as WTs and PVs, their output power during operation cannot exceed their maximum generation power, as shown in (39).

$$0 \leq P_{i,y,d,t} \leq p_{i,y,d,t} \cdot Cap_{i,y}^{total} \quad \forall i \in \Omega^{RE}, y \in [1, 8], d \in D, t \in T \quad (39)$$

### 10) Operation Constraints of FCs

Since the FC possesses a millisecond-second dynamic response speed [30], [31], it can be modeled without considering the start-up/shut-down constraints and ramping constraints, and the output power is shown in (40).

$$0 \leq P_{i,y,d,t} \leq Cap_{i,y}^{total} \quad \forall i \in \Omega^{FC}, y \in [1, 8], d \in D, t \in T \quad (40)$$

### 11) Operation Constraints of Energy Storage

Here, we only consider PS and BS as storage devices for intraday regulation. In the planning phase, both are often modeled similarly and differ only in specific parameters [14]. Formulas (41) and (42) constrain the charging/discharging power and storage capacity of the energy storage, respectively. Formula (43) characterizes the time continuity of the change in the storage capacity, and (44) ensures that the storage capacity achieves the short-term intraday balance.

$$\begin{cases} 0 \leq P_{i,y,d,t}^{dis} \leq Cap_{i,y}^{total} \\ 0 \leq P_{i,y,d,t}^{ch} \leq Cap_{i,y}^{total} \end{cases} \quad \forall i \in \{\Omega^{BS}, \Omega^{PS}\}, y \in [1, 8], d \in D, t \in T \quad (41)$$

$$0 \leq S_{i,y,d,t} \leq T_i \cdot Cap_{i,y}^{total} \quad \forall i \in \{\Omega^{BS}, \Omega^{PS}\}, y \in [1, 8], d \in D, t \in T \quad (42)$$

$$S_{i,y,d,t} = S_{i,y,d,t-1} + \eta_i^{ch} P_{i,y,d,t}^{ch} - \frac{P_{i,y,d,t}^{dis}}{\eta_i^{dis}} \quad \forall i \in \{\Omega^{BS}, \Omega^{PS}\}, y \in [1, 8], d \in D, t \in T \quad (43)$$

$$S_{i,y,d,t} = S_{i,y,d,T_{max}} = 0.5 \cdot Cap_{i,y}^{total} \quad \forall i \in \{\Omega^{BS}, \Omega^{PS}\}, y \in [1, 8], d \in D \quad (44)$$

### 12) Constraints of Spinning Reserve

The unpredictability of loads and renewable energy outputs will lead to power imbalances. Consequently, ensuring sufficient spinning reserve capacity is essential to maintain a balance between power generation and load. In the PPEP model, we only consider generation units that can adjust to the required output within 10 min to participate in the spinning reserve, as shown in (45).

$$\sum_{i \in \Omega^{GU} \cup \Omega^{RE}} P_{i,y,d,t}^{sr} + \sum_{j \in \Omega^{DC,rec}} P_{j,y,d,t}^{sr} \geq \tau_{load} \left( L_{i,y,d,t} + \sum_{j \in \Omega^{DC,send}} P_{j,y,d,t} \right) + \tau_{RE} \sum_{i \in \Omega^{RE}} P_{i,y,d,t} \quad \forall y \in [1, 8], d \in D, t \in T \quad (45)$$

Further, the capacity of each type of generation unit that can provide spinning reserve is represented by (46)-(53).

$$0 \leq P_{i,y,d,t}^{sr} \leq P_{i,y,d,t}^{on} - P_{i,y,d,t} \quad \forall i \in \Omega^{TG}, y \in [1, 8], d \in D, t \in T \quad (46)$$

$$0 \leq P_{i,y,d,t}^{sr} \leq P_{i,y,d,t}^{on} - P_{i,y,d,t}^{net} \quad \forall i \in \Omega^{CTG}, y \in [1, 8], d \in D, t \in T \quad (47)$$

$$0 \leq P_{i,y,d,t}^{sr} \leq \delta_i^{rp} P_{i,y,d,t}^{on} \quad \forall i \in \{\Omega^{TG}, \Omega^{CTG}\}, y \in [1, 8], d \in D, t \in T \quad (48)$$

$$0 \leq P_{i,y,d,t}^{sr} \leq Cap_{i,y}^{total} - P_{i,y,d,t} \quad \forall i \in \{\Omega^{BG}, \Omega^{HG}, \Omega^{NG}, \Omega^{FC}\}, y \in [1, 8], d \in D, t \in T \quad (49)$$

$$0 \leq P_{i,y,d,t}^{sr} \leq Cap_{i,y}^{total} - P_{i,y,d,t}^{net} \quad \forall i \in \Omega^{CBG}, y \in [1, 8], d \in D, t \in T \quad (50)$$

$$0 \leq P_{i,y,d,t}^{sr} \leq Cap_{i,y}^{total} - P_{i,y,d,t}^{dis} + P_{i,y,d,t}^{ch} \quad \forall i \in \{\Omega^{BS}, \Omega^{PS}\}, y \in [1, 8], d \in D, t \in T \quad (51)$$

$$0 \leq P_{i,y,d,t}^{sr} \leq 6S_{i,y,d,t} \eta_i^{dis} \quad \forall i \in \{\Omega^{BS}, \Omega^{PS}\}, y \in [1, 8], d \in D, t \in T \quad (52)$$

$$0 \leq P_{j,y,d,t}^{sr} \leq Cap_{j,y}^{total} - P_{j,y,d,t}^{DC,rec} \quad \forall j \in \Omega^{DC,rec}, y \in [1, 8], d \in D, t \in T \quad (53)$$

where  $6S_{i,y,d,t} \eta_i^{dis}$  denotes the maximum power that energy storage device  $i$  can release within 10 min [14].

Notably, (53) indicates that the remaining capacity of the transmission lines limits the spinning reserve capacity that DC transmission lines can provide. In the PPEP model, the possibility of providing spinning reserve capacity by ACLs is not considered due to the difficulty in scheduling ACL power flows within 10 min.

### C. Objective Function

The objective of the PPEP model is to minimize the total cost at each stage of the system, encompassing capital, maintenance, and operation costs. Using 2020 as the reference year, we analyze the total costs of 8 stages from 2025 to 2060, with a 5-year interval, as depicted in (54).

$$\min COST = \sum_{y=1}^8 \frac{C_y^{inv} + C_y^{mat} + C_y^{op}}{(1+r)^{5y}} \quad (54)$$

The total capital, maintenance, and operation costs can be calculated as shown in (55)-(57), respectively.

$$C_y^{inv} = \sum_{i \in \Omega^{GT}} \left\{ \left[ \sum_{x=1}^{45-5y} (1+r)^{-x} \right] \frac{r}{1-(1+r)^{-N_{i,y}}} c_{i,y}^{inv} \Delta Cap_{i,y}^{inc} \right\} \quad (55)$$

$$C_y^{mat} = \sum_{i \in \Omega^{GT}} \left\{ \left[ \sum_{x=1}^5 (1+r)^{-x} \right] c_{i,y}^{mat} Cap_{i,y}^{total} \right\} \quad \forall y \in [1, 8] \quad (56)$$

$$C_y^{op} = \frac{5 \times 8760}{D_{max} T_{max}} \left[ \sum_{i \in \Omega^{GT}} \sum_{d \in D} \sum_{t \in T} (c_i^{yop} P_{i,y,d,t} + c_i^{su} P_{i,y,d,t}^{su} + c_i^{sd} P_{i,y,d,t}^{sd}) + \sum_{i \in \Omega^{CTG}, \Omega^{CBG}} \sum_{d \in D} \sum_{t \in T} c_i^{ccs} E_{i,y,d,t}^{ccs} + \sum_{i \in \Omega^{GT}} \sum_{d \in D} \sum_{t \in T} c_y^{car} (e_i P_{i,y,d,t} - E_{i,y,d,t}^{ccs}) + \sum_{d \in D} \sum_{t \in T} c_y^{shed} P_{y,d,t}^{shed} \right] \quad \forall y \in [1, 8] \quad (57)$$

where  $\left[ \sum_{x=1}^{45-5y} (1+r)^{-x} \right] \frac{r}{1-(1+r)^{-N_{i,y}}}$  is intended to discount the overnight investment cost of unit  $i$  at stage  $y$  to the capital cost over the planning period [14].

In summary, since binary variables are introduced in the model, the PPEP model proposed in this paper is a mixed-integer linear programming (MILP) model, which can be solved by invoking the Gurobi/Cplex solver directly. The simulation environment here is CPU i7-13700k, RAM 32 GB, and Gurobi version 9.5.2.

## IV. DESIGN OF MMTE MECHANISM

To address the lack of operation incentives for coal-based units compared with renewable-based units in power systems rich in renewable energy generation, this section proposes an innovative solution known as the MMTE mechanism. With the MMTE mechanism, the coal-based units can participate in the energy and ancillary service markets, while the renewable-based units can participate in the energy market. The MMTE mechanism guarantees that the profits of both are equitably met.

Considering that the renewable-based unit has the characteristics of stochastic output and low inertia, it only profits from the sale of electricity through the energy market. In contrast, the coal-based unit has a stable and controllable output, which can participate in both the sale of electricity in the energy market and reserve in the ancillary service market for profit.

Further, considering that coal-based units undertake the reserve role of renewable-based units, their profitability through the ancillary service market should be paid by the operators of the renewable-based units. The equilibrium of interests between renewable-based and coal-based units can be achieved through reasonable market trading.

Note that due to the variability in the installed capacity of renewable-based and coal-based units, the equilibrium of interests here refers to the average profit per unit capacity.

Equation (58) calculates the equilibrium of interests between renewable-based and coal-based units.

$$\frac{REV_y^{RE}}{\sum_{i \in \Omega^{RE}} Cap_{i,y}^{total}} = \frac{REV_y^{COAL}}{\sum_{i \in \{\Omega^{TG}, \Omega^{CTG}\}} Cap_{i,y}^{total}} \quad \forall y \in [1, 8] \quad (58)$$

The net revenues of the renewable-based and coal-based units can be further expressed as (59) and (60), respectively.

$$REV_y^{RE} = REV_y^{RE,ELE} - REV_y^{COAL,sr} - REV_y^{COAL,nsr} \quad \forall y \in [1, 8] \quad (59)$$

$$REV_y^{COAL} = REV_y^{COAL,ELE} + REV_y^{COAL,sr} + REV_y^{COAL,nsr} \quad \forall y \in [1, 8] \quad (60)$$

Specifically, the above revenues can be calculated by (61)-(64).

$$REV_y^{RE,ELE} = (\lambda_y^{grid} - LCOE_y^{RE}) \sum_{i \in \Omega^{RE}} \sum_{d \in D} \sum_{t \in T} P_{i,y,d,t} \quad \forall y \in [1, 8] \quad (61)$$

$$REV_y^{COAL,ELE} = (\lambda_y^{grid} - LCOE_y^{COAL}) \sum_{d \in D} \sum_{t \in T} \left( \sum_{i \in \Omega^{TG}} P_{i,y,d,t} + \sum_{i \in \Omega^{CTG}} P_{i,y,d,t}^{net} \right) \quad \forall y \in [1, 8] \quad (62)$$

$$REV_y^{COAL,sr} = \lambda_y^{sr} \sum_{d \in D} \sum_{t \in T} \sum_{i \in \{\Omega^{TG}, \Omega^{CTG}\}} P_{i,y,d,t}^{sr} \quad \forall y \in [1, 8] \quad (63)$$

$$REV_y^{COAL,nsr} = \lambda_y^{nsr} \sum_{d \in D} \sum_{t \in T} \sum_{i \in \{\Omega^{TG}, \Omega^{CTG}\}} (Cap_{i,y}^{total} - P_{i,y,d,t}^{on}) \quad \forall y \in [1, 8] \quad (64)$$

Further,  $LCOE_y^{COAL}$  and  $LCOE_y^{RE}$  are obtained by (65) and (66), respectively.

$$LCOE_y^{COAL} = \frac{D_{\max} T_{\max} \sum_{i \in \{\Omega^{TG}, \Omega^{CTG}\}} (C_{i,y}^{inv} + C_{i,y}^{mat} + C_{i,y}^{op})}{8760 \sum_{d \in D} \sum_{t \in T} \left( \sum_{i \in \Omega^{TG}} P_{i,y,d,t} + \sum_{i \in \Omega^{CTG}} P_{i,y,d,t}^{net} \right)} \quad \forall y \in [1, 8] \quad (65)$$

$$LCOE_y^{RE} = \frac{D_{\max} T_{\max} \sum_{i \in \Omega^{RE}} (C_{i,y}^{inv} + C_{i,y}^{mat} + C_{i,y}^{op})}{8760 \sum_{d \in D} \sum_{t \in T} \sum_{i \in \Omega^{RE}} P_{i,y,d,t}} \quad \forall y \in [1, 8] \quad (66)$$

For the coal-based and renewable-based units, we can calculate  $C_{i,y}^{inv}$  and  $C_{i,y}^{mat}$  using (67) and (68), respectively. However, the calculation of  $C_{i,y}^{op}$  for the coal-based and renewable-based units is different, as represented by (69) and (70), respectively.

$$C_{i,y}^{inv} = \kappa_i c_{i,y}^{inv} Cap_{i,y}^{total} \quad \forall i \in \{\Omega^{TG}, \Omega^{CTG}, \Omega^{RE}\}, y \in [1, 8] \quad (67)$$

$$C_{i,y}^{mat} = c_{i,y}^{mat} Cap_{i,y}^{total} \quad \forall i \in \{\Omega^{TG}, \Omega^{CTG}, \Omega^{RE}\}, y \in [1, 8] \quad (68)$$

$$C_{i,y}^{op} = \frac{8760}{D_{\max} T_{\max}} \sum_{d \in D} \sum_{t \in T} [c_i^{vop} P_{i,y,d,t} + c_i^{su} P_{i,y,d,t}^{su} + c_i^{sd} P_{i,y,d,t}^{sd} + c_i^{ccs} E_{i,y,d,t}^{ccs} + c_i^{car} (e_i P_{i,y,d,t} - E_{i,y,d,t}^{ccs})] \quad \forall i \in \{\Omega^{TG}, \Omega^{CTG}\}, y \in [1, 8] \quad (69)$$

$$C_{i,y}^{op} = \frac{8760}{D_{\max} T_{\max}} \sum_{d \in D} \sum_{t \in T} c_i^{vop} P_{i,y,d,t} \quad \forall i \in \Omega^{RE}, y \in [1, 8] \quad (70)$$

where  $\kappa_i = \frac{r(1+r)^{N_{i,y}}}{(1+r)^{N_{i,y}} - 1}$  is the capital conversion factor used

to convert whole-life capital costs to annual capital costs.

Notably, after acquiring the power expansion planning results for each stage based on the PPEP model, the variables in (58)-(70) are  $\lambda_y^{grid}$ ,  $\lambda_y^{sr}$ , and  $\lambda_y^{nsr}$ . Therefore, the value of one variable can be solved based on the given values of the other two. As shown in Algorithm 1, to further illustrate the solution process of the MMTE mechanism, we give the solution of  $\lambda_y^{nsr}$  when  $\lambda_y^{grid}$  and  $\lambda_y^{sr}$  are assumed to be known.

---

**Algorithm 1:** solution process of MMTE mechanism
 

---

*Step 1:* set the initial values of  $\lambda_y^{grid}$  and  $\lambda_y^{sr}$ .

*Step 2:* calculate the LCOE of renewable-based and coal-based units through (65)-(70).

*Step 3:* calculate the revenues of renewable-based and coal-based units in the energy market through (61) and (62), respectively.

*Step 4:* calculate the revenue of coal-based units for providing spinning reserve service through (63).

*Step 5:* calculate the revenue of coal-based units for providing non-spinning reserve service with the variable  $\lambda_y^{nsr}$  through (64).

*Step 6:* calculate the net revenues of renewable-based and coal-based units with the variable  $\lambda_y^{nsr}$  through (59) and (60), respectively.

*Step 7:* solve (58) to obtain the value of  $\lambda_y^{nsr}$ .

*Step 8:* if  $0 \leq \lambda_y^{nsr} \leq \lambda_y^{sr}$ , return  $\lambda_y^{nsr}$  and terminate; else, go to *Step 9*.

*Step 9:* change the values of  $\lambda_y^{grid}$  and  $\lambda_y^{sr}$ , go to *Step 2*.

---

## V. CASE STUDY

## A. Scenario Setting

National policies profoundly affect the power system planning, and under the global carbon neutrality goal, carbon emissions will be a crucial factor affecting power system

planning. Based on different targets or agreements, [14] predicted the carbon emission limits at various stages in China under the following four scenarios.

1) Business-as-usual (BAU): not considering carbon emission limitations.

2) Nationally determined contribution (NDC): calculating carbon emission limitations based on the Paris Agreement.

3) Global warming of 2.0 °C (GM2.0): calculating carbon emission limitations based on the Intergovernmental Panel on Climate Change (IPCC) goal of global average surface warming of no more than 2.0 °C.

4) Carbon neutrality (CN2050): calculating carbon emission limitations based on that the whole power system achieves carbon neutrality in 2050, which also meets the IPCC goal of global average surface warming of no more than 1.5 °C.

Taking Xinjiang, China, as a case study, based on China's carbon emission limitation projections, we calculate the carbon emission limitation at various stages in different scenarios in Xinjiang, China, according to the share of Xinjiang's power load in the national power load, as shown in Fig. 2.

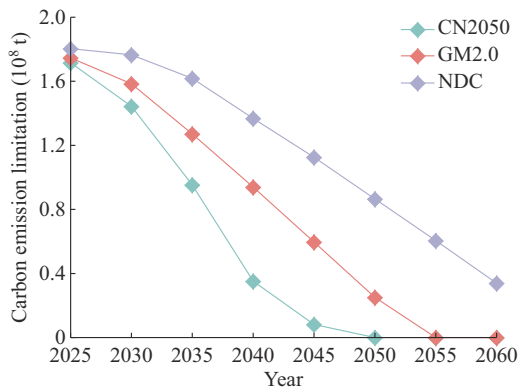


Fig. 2. Carbon emission limitations in Xinjiang, China, under different scenarios.

Note that, to balance the generalizability of the results with the degree of conservatism in carbon emission policies, subsequent results are derived based on the GM2.0 scenario unless otherwise stated.

### B. Data and Parameters

Table II shows the installed capacities of generation units and transmission lines in Xinjiang, China, in 2020 [32], i.e., the reference year, for power expansion planning. Table III further provides installed capacities of TGs and CCUS-TGs with different stand-alone capacities in Xinjiang, China, in 2020, to model the construction and retirement accurately with different stand-alone capacities [33], [34]. In addition, other parameters and data related to the case study can be found in [35].

### C. Selection of Typical Days

The PPEP model is a large-scale MILP problem, which is difficult to be solved using 8760-hour time series throughout one year. Therefore, it is necessary to adopt appropriate time-series reduction techniques.

TABLE II  
INSTALLED CAPACITIES OF GENERATION UNITS AND TRANSMISSION LINES IN XINJIANG, CHINA, IN 2020

Type	Installed capacity (GW)	Type	Installed capacity (GW)
Cen-PV	11.854	HG	7.108
Dis-PV	0.205	FC	0
On-WT	23.552	BS	3.670
Off-WT	0	PS	1.200
BG	1.098	ACL	10.000
CCUS-BG	0.122	DCRL	0
NG	0	DCSL	20.000

TABLE III  
INSTALLED CAPACITIES OF TGs AND CCUS-TGs WITH DIFFERENT STAND-ALONE CAPACITIES IN XINJIANG, CHINA, IN 2020

Stand-alone capacity (MW)	Installed capacity (GW)	
	TG	CCUS-TG
< 100	2.10	0
100-200	7.35	0
200-300	1.62	0
300-600	27.96	0
600-1000	16.54	0
> 1000	2.20	0

In order to maintain the original time-series coupling characteristics while considering the solution speed, we use the soft-DTW-based  $K$ -medoids technique for the selection of typical days [36], [37], and select the optimal number of typical days based on the elbow method [38].

Figure 3 gives the distortion value under different cluster numbers. The optimal cluster number is determined when the degree of reduction of the distortion value starts to remain relatively smooth. Here, 6 and 11 are both appropriate cluster numbers. Considering the accuracy and the complexity of the PPEP model, we select 11 as the optimal number of typical days for planning.

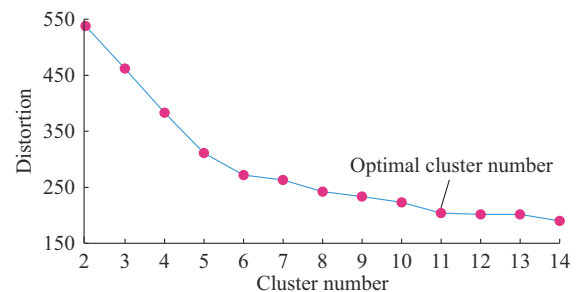


Fig. 3. Distortion value under different cluster numbers.

### D. Power Expansion Planning Results

The installed capacities of different power supplies in Xinjiang, China, is detailed in Fig. 4(a), covering various stages of development. The primary power sources will be Cen-PV and On-WT, with the total installed capacity expected to increase from 35.41 GW in 2020 to 645.45 GW in 2060. Un-

fortunately, Dis-PV and Off-WT will not be installed due to geographical limitations and resource endowment.

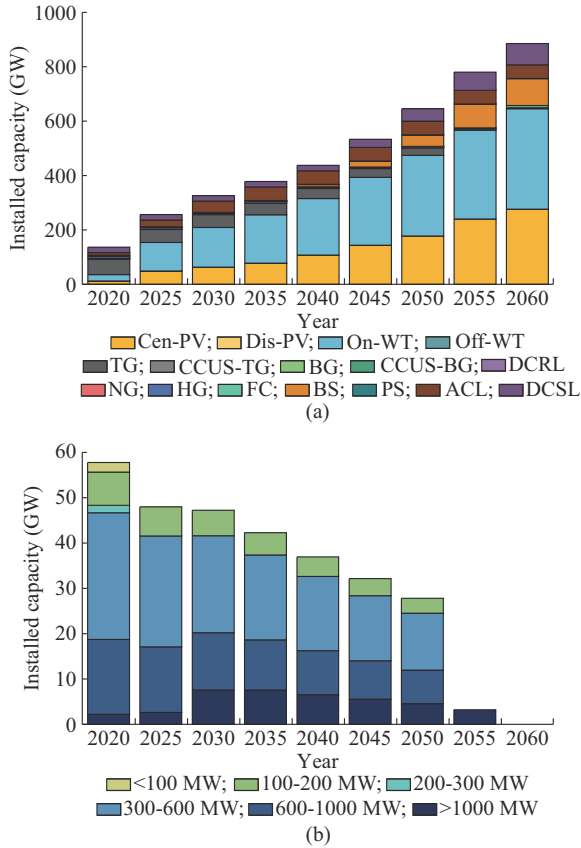


Fig. 4. Power and transmission installation plan in Xinjiang, China. (a) Installed capacities of different power supplies. (b) Stand-alone capacities of TGs.

The installed capacity of TGs will gradually decrease as they are phasing out. Furthermore, 2050 is the critical stage when 24.6 GW TGs will be retired, leaving only 3.22 GW as backup power to support the operation of the power systems rich in renewable energy generation, and the full retirement of TGs will be realized in 2060. In particular, CCUS-TG will not be cost-competitive and thus will not be installed at any further stage. Moreover, the capacity of BS will be increased from 3.67 GW in 2020 to 98.74 GW in 2060 due to the need for large-scale energy storage to maintain power supply stability with high renewable energy penetration. Notably, FC starts to be cost-competitive in 2060 due to technological advances and cost reductions, and its installed capacity will reach 8.33 GW, an increase of about 873% compared with 2055.

The installed capacities of ACL and DCSL will experience rapid growth. The installed capacities of ACL are expected to reach the maximum planning capacity (50 GW) in 2035. Meanwhile, the capacity of DCSL will exceed 70 GW in 2060. However, DCRL will not be constructed. Additionally, BG, CCUS-BG, NG, HG, and PS will have relatively limited installed capacities over the years and serve mainly as supplementary power sources.

Figure 4(b) shows the stand-alone capacities of TGs

(CCUS-TG will not be installed at any further stage and is not analyzed here). Overall, the total installed capacity of TG shows a decreasing trend from 57.77 GW in 2020 to full retirement in 2060. The most significant retirement occurs between 2050 and 2055, with 88% of the installed capacity in 2050 being retired. However, the retirement trend varies for TGs with different stand-alone capacities. TGs with smaller stand-alone capacities will be phased out, while those with stand-alone capacities greater than 1000 MW will increase before decreasing. Specifically, TGs with stand-alone capacity greater than 1000 MW will reach a peak installed capacity of 7.55 GW in 2035 before full retirement in 2060. On the one hand, TGs with larger stand-alone capacities will gradually replace those with smaller stand-alone capacities for power supply due to economy and efficiency advantages. Thus, their installed capacity will go through a growth stage. On the other hand, with a high proportion of renewable energy penetration in the future, TGs will shift from power generation to capacity reserve roles, and thus their installed capacity will decrease.

*E. Scheduling Results on Typical Days*

Figure 5 presents the hourly scheduling curves for all power sources and power loads on typical days in 2030, 2045, and 2060. As time progresses, the outputs of generation units (excluding TG) increase due to the rise in power load. However, as renewable energy penetration increases, the output power of TGs and its share will decrease.

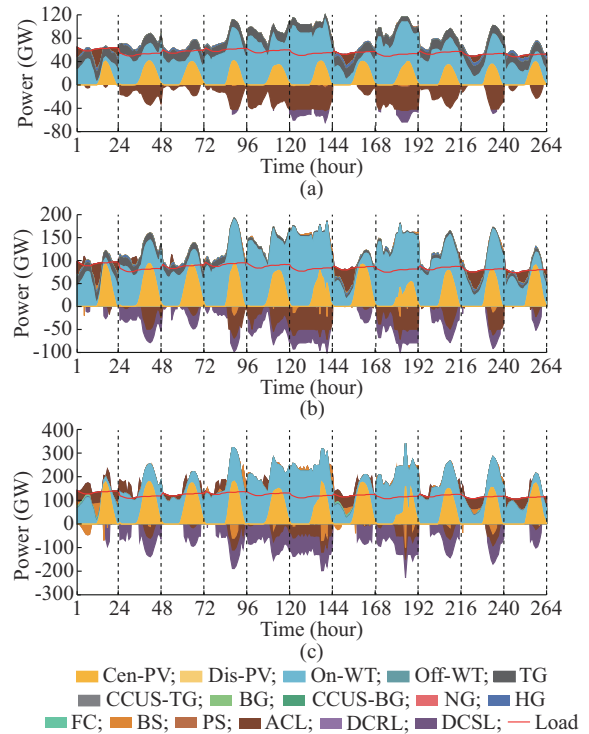


Fig. 5. Hourly scheduling curves for all power sources and power loads. (a) 2030. (b) 2045. (c) 2060.

Regarding power deliveries, Xinjiang, China, primarily sends power through ACL in 2030. However, power sent

through DCSL increases as annual power generation increases and becomes similar to that sent through ACL in 2060. After ACL expands to its capacity limit, the excess power transmission demand can only be met through DCSL. The frequency and amount of charging and discharging of BS will significantly increase in 2060 compared with that in 2030 due to the increase in the installed capacity of BS.

Due to flexibility and economic constraints, the output power of TG is stable on a typical day. Furthermore, the BS primarily charges during the period with Cen-PV power surplus (14:00-22:00) and discharges during period with the Cen-PV and On-WT power deficit (08:00-14:00) to achieve flexible regulation and maintain power balance. Meanwhile, AC sends power out most of the time and receives power to compensate for the deficit in a few hours (08:00-14:00). Other power sources are less powerful and not used as the primary power sources.

In addition, as time progresses, the constraints on renewable energy penetration result in a mismatch between the output power of TG and the variation of the power load, leading to a tremendous source-load power imbalance, mainly compensated by the renewable-based units, the ACL, and the BS. In particular, FC also carries part of the generation in 2060 (typical days 1 and 7), revealing the potential value of hydrogen in the generation sector in the future.

## F. MMTE Mechanism Elements

### 1) LCOE Assessment

The primary goal of the MMTE mechanism is to achieve the equilibrium of interests between thermal-based and renewable-based units. To determine whether to implement the MMTE mechanism, evaluating the LCOE for both power unit types is crucial.

To illustrate the necessity of implementing the MMTE mechanism, we calculate the LCOE versus vintage curves for coal-based units (including TG and CCUS-TG) and renewable-based units (including Cen-PV, Dis-PV, On-WT, and Off-WT) in four carbon emission limitation scenarios, as presented in Fig. 6.

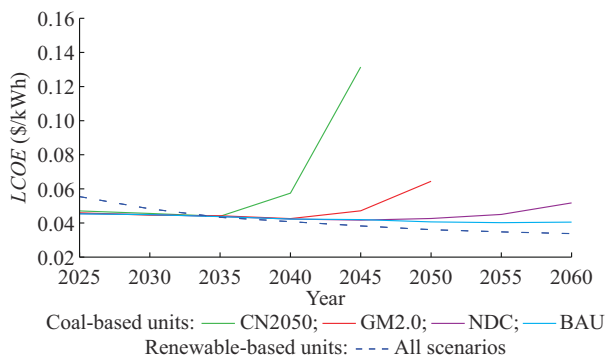


Fig. 6. LCOE of coal-based and renewable-based units from 2025 to 2060 in four carbon emission limitation scenarios.

Notably, due to the zero carbon emission constraint, the LCOE for coal-based units in the CN2050 and GM2.0 scenarios will be missing for years when coal-based units are phased out. In addition, since renewable-based units do not produce any carbon emissions from power generation, their

LCOE curves highly overlap in all the scenarios. On the contrary, progressively more challenging restrictions on carbon emission policy will significantly increase the LCOE of coal-based units.

The LCOE of renewable-based units decreases over time, from 0.0554 \$/kWh in 2025 to 0.0335 \$/kWh in 2060, while the LCOE of coal-based units rises under all the scenarios. In particular, the LCOE of coal-based units is lower than that of renewable-based units until 2035. The situation will be reversed after 2035, and the more stringent the carbon emission limitations, the higher the LCOE of coal-based units.

Overall, due to the carbon emission limitations, the LCOE of coal-based units will exceed that of renewable-based units after 2035. In order to continue to incentivize the operation of coal-based units, appropriate financial compensation must be provided, highlighting the need for the MMTE mechanism proposed in this paper.

### 2) Analysis of MMTE Mechanism

The above study has pointed out that the LCOE of coal-based units will be higher than that of renewable-based units after 2035. Therefore, we only consider the equilibrium of interests between them through the MMTE mechanism after 2035. Figure 7 shows the pricing relationships between grid-connected prices, spinning reserve prices, and non-spinning reserve prices at each stage from 2035 to 2060 in the GM2.0 scenario.

Notably, in practice, the non-spinning reserve price should be lower than the spinning reserve price and should never be negative. Therefore, we have excluded the gray areas in Fig. 7 that indicate negative values for non-spinning reserve prices, as well as the gray areas with diagonal lines that indicate the non-spinning reserve prices exceed the spinning reserve prices.

Overall, on the one hand, the impact of spinning reserve prices on the equilibrium of interests between coal-based and renewable-based units gradually decreases over time, and the opposite is true for grid-connected prices; on the other hand, the feasible domain for non-spinning reserve prices first increases and then decreases over time. The former is due to the gradual shift of coal-based units from generation and spinning reserve to non-spinning reserve roles, while the latter is affected by the dual impact of changes in the installed capacities and LCOE of coal-based units.

Specifically, the changes in the pricing relationship among the three prices can be divided into three stages.

1) Stage 1 (from 2035 to 2045): the non-spinning reserve price has the opposite trend to the grid-connected price and the spinning reserve price; the grid-connected price has a more significant impact on the non-spinning reserve price than the spinning reserve price; and the feasible domain of the non-spinning reserve price is gradually increasing.

2) Stage 2 (from 2045 to 2055): the non-spinning reserve price is positively correlated with the grid-connected price; the spinning reserve price does not affect the non-spinning reserve price; and the feasible domain of non-spinning reserve price gradually decreases.

3) Stage 3 (from 2055 to 2060): coal-based units are fully retired, and the MMTE mechanism loses its role.

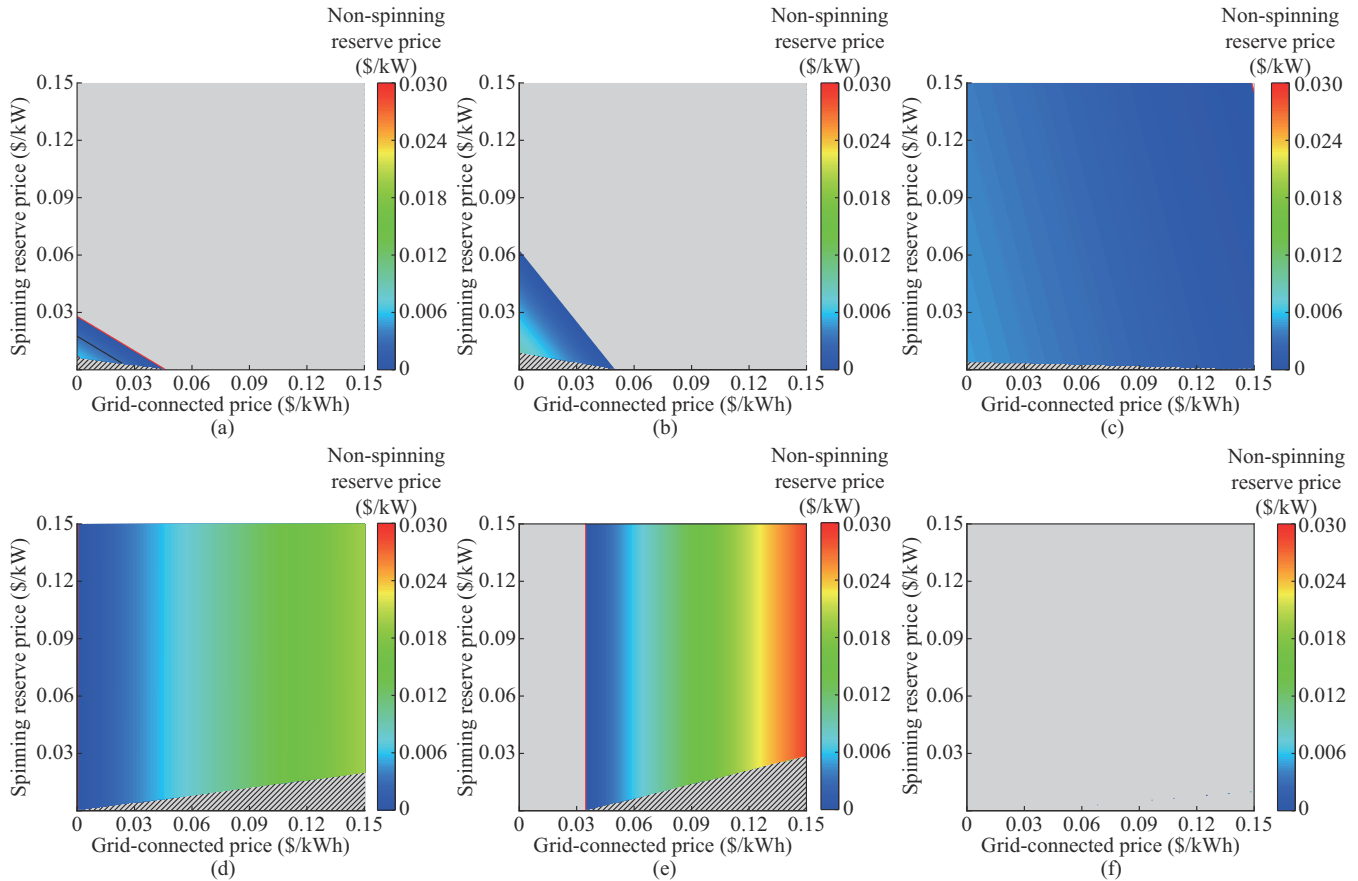


Fig. 7. Pricing relationships among grid-connected prices, spinning reserve prices, and non-spinning reserve prices from 2035 to 2060 in GM2.0 scenario. (a) 2035. (b) 2040. (c) 2045. (d) 2050. (e) 2055. (f) 2060.

The reasons for the above changes are as follows.

At Stage 1, the LCOE gap between coal-based and renewable-based units widens over time, the feasible domain of non-spinning reserve price increases, the gradual retirement of coal-based units reduces the spinning reserve capacity, and the impact of spinning reserve price decreases.

At Stage 2, the coal-based units gradually reduce the provision of spinning reserve capacity, the non-spinning reserve price is mainly affected by the grid-connected price, and the higher grid-connected price increases the revenue of the renewable-based units. In order to equalize the benefits, the non-spinning reserve price will also increase. In particular, in 2055, when coal-based units no longer provide spinning reserve and power generation services, their revenues come only from the non-spinning reserve paid by renewable-based units. Both will lose their revenues when the grid-connected price is lower than the LCOE of renewable-based units. Thus, the feasibility domain is further reduced.

At Stage 3, the coal-based units are wholly retired, so the MMTE mechanism no longer works.

The MMTE mechanism outlined in this paper offers promising potential for balancing the revenue streams of both coal-based and renewable-based units, especially at Stages 1 and 2. By maximizing the profit of energy and ancillary service markets of coal-based units, the MMTE mechanism can effectively boost the incentive for such units to participate in the market. Ultimately, this can establish a more equitable landscape for coal-based and renewable-based units.

## VI. CONCLUSION

This paper proposes the PPEP model for energy transition planning and the MMTE mechanism to realize equilibrium of interests between coal-based and renewable units while improving the motivation of coal-based units to participate in the energy and ancillary service market. The conclusions are obtained as follows.

1) Taking Xinjiang, China, as an example, the installed capacities of renewable-based units will reach 645.45 GW in 2060, requiring 98.74 GW of BS to be deployed to smooth load fluctuations, and FC will be cost-competitive in 2060.

2) The retirement of TGs with smaller stand-alone capacity units is set to commence. The stand-alone capacity of over 1000 MW is projected to increase to 7.55 GW by 2035 before retirement in 2060.

3) The LCOE of coal-based units will be higher than that of renewable-based units after 2035, and the more stringent the carbon emission policy limitations, the higher the LCOE of coal-based units.

4) The results of the MMTE mechanism in Xinjiang, China, indicate that the pricing of grid-connected prices, spinning reserve prices, and non-spinning reserve prices will go through three stages and the MMTE mechanism can effectively equalize the interests of coal-based and renewable-based units, especially before 2055.

## REFERENCES

- [1] X. Yang, B. Cai, and Y. Xue, "Review on optimization of nuclear power development: a cyber-physical-social system in energy perspective," *Journal of Modern Power Systems and Clean Energy*, vol. 10, no. 3, pp. 547-561, May 2022.
  - [2] S. Chen, H. Mi, J. Ping *et al.*, "A blockchain consensus mechanism that uses proof of solution to optimize energy dispatch and trading," *Nature Energy*, vol. 7, pp. 495-502, Jun. 2022.
  - [3] X. Chen, J. Lv, M. B. McElroy *et al.*, "Power system capacity expansion under higher penetration of renewables considering flexibility constraints and low carbon policies," *IEEE Transactions on Power Systems*, vol. 33, no. 6, pp. 6240-6253, Nov. 2018.
  - [4] Z. Gu, G. Pan, W. Gu *et al.*, "Robust optimization of scale and revenue for integrated power-to-hydrogen systems within energy, ancillary services, and hydrogen markets," *IEEE Transactions on Power Systems*, vol. 39, no. 3, pp. 5008-5023, Oct. 2023.
  - [5] C. Li, N. Wang, X. Shen *et al.*, "Energy planning of Beijing towards low-carbon, clean and efficient development in 2035," *CSEE Journal of Power and Energy Systems*, doi: 10.17775/CSEEJPES.2021.03620
  - [6] M. Alraddadi, A. J. Conejo, and R. M. Lima, "Expansion planning for renewable integration in power system of regions with very high solar irradiation," *Journal of Modern Power Systems and Clean Energy*, vol. 9, no. 3, pp. 485-494, May 2021.
  - [7] X. Wang, M. Shahidehpour, C. Jiang *et al.*, "Coordinated planning strategy for electric vehicle charging stations and coupled traffic-electric networks," *IEEE Transactions on Power Systems*, vol. 34, no. 1, pp. 268-279, Jan. 2019.
  - [8] A. S. Brouwer, M. van den Broek, W. Zappa *et al.*, "Least-cost options for integrating intermittent renewables in low-carbon power systems," *Applied Energy*, vol. 161, pp. 48-74, Jan. 2016.
  - [9] M. Pehl, A. Arvesen, F. Humpenöder *et al.*, "Understanding future emissions from low-carbon power systems by integration of life-cycle assessment and integrated energy modelling," *Nature Energy*, vol. 2, pp. 939-945, Dec. 2017.
  - [10] M. Qadrdan, M. Chaudry, N. Jenkins *et al.*, "Impact of transition to a low carbon power system on the GB gas network," *Applied Energy*, vol. 151, pp. 1-12, Aug. 2015.
  - [11] M. Zeyringer, J. Price, B. Fais *et al.*, "Designing low-carbon power systems for Great Britain in 2050 that are robust to the spatiotemporal and inter-annual variability of weather," *Nature Energy*, vol. 3, pp. 395-403, Apr. 2018.
  - [12] G. He, J. Lin, F. Sifuentes *et al.*, "Rapid cost decrease of renewables and storage accelerates the decarbonization of China's power system," *Nature Communications*, vol. 11, p. 2486, May 2020.
  - [13] X. Chen, Y. Liu, Q. Wang *et al.*, "Pathway toward carbon-neutral electrical systems in China by mid-century with negative CO<sub>2</sub> abatement costs informed by high-resolution modeling," *Joule*, vol. 5, no. 10, pp. 2715-2741, Oct. 2021.
  - [14] Z. Zhuo, E. Du, N. Zhang *et al.*, "Cost increase in the electricity supply to achieve carbon neutrality in China," *Nature Communications*, vol. 13, no. 1, p. 3172, Jun. 2022.
  - [15] S. Tan, X. Wang, and C. Jiang, "Dual interval optimization based trading strategy for ESCO in day-ahead market with bilateral contracts," *Journal of Modern Power Systems and Clean Energy*, vol. 8, no. 3, pp. 582-590, May 2020.
  - [16] M. Yan, M. Shahidehpour, A. Alabdulwahab *et al.*, "Blockchain for transacting energy and carbon allowance in networked microgrids," *IEEE Transactions on Smart Grid*, vol. 12, no. 6, pp. 4702-4714, Nov. 2021.
  - [17] M. Yan, M. Shahidehpour, A. Paaso *et al.*, "Distribution network-constrained optimization of peer-to-peer transactive energy trading among multi-microgrids," *IEEE Transactions on Smart Grid*, vol. 12, no. 2, pp. 1033-1047, Mar. 2021.
  - [18] S. Chen, Z. Shen, L. Zhang *et al.*, "A trusted energy trading framework by marrying blockchain and optimization," *Advances in Applied Energy*, vol. 2, p. 100029, May 2021.
  - [19] E. Ela, V. Gevorgian, A. Tuohy *et al.*, "Market designs for the primary frequency response ancillary service – part I: motivation and design," *IEEE Transactions on Power Systems*, vol. 29, no. 1, pp. 421-431, Jan. 2014.
  - [20] D. J. Shiltz, M. Cvetković, and A. M. Annaswamy, "An integrated dynamic market mechanism for real-time markets and frequency regulation," *IEEE Transactions on Sustainable Energy*, vol. 7, no. 2, pp. 875-885, Apr. 2016.
  - [21] Z. Guo, P. Pinson, S. Chen *et al.*, "Chance-constrained peer-to-peer joint energy and reserve market considering renewable generation uncertainty," *IEEE Transactions on Smart Grid*, vol. 12, no. 1, pp. 798-809, Jan. 2021.
  - [22] Y. Yang, J. Peng, and Z. Ye, "A market clearing mechanism considering primary frequency response rate," *IEEE Transactions on Power Systems*, vol. 36, no. 6, pp. 5952-5955, Nov. 2021.
  - [23] B. K. Poolla, S. Bolognani, N. Li *et al.*, "A market mechanism for virtual inertia," *IEEE Transactions on Smart Grid*, vol. 11, no. 4, pp. 3570-3579, Jul. 2020.
  - [24] Z. Liang, R. Mieth, and Y. Dvorkin, "Inertia pricing in stochastic electricity markets," *IEEE Transactions on Power Systems*, vol. 38, no. 3, pp. 2071-2084, May 2023.
  - [25] J. Hu, Z. Yan, X. Xu *et al.*, "Inertia market: mechanism design and its impact on generation mix," *Journal of Modern Power Systems and Clean Energy*, vol. 11, no. 3, pp. 744-756, May 2023.
  - [26] K. Li, H. Guo, X. Fang *et al.*, "Market mechanism design of inertia and primary frequency response with consideration of energy market," *IEEE Transactions on Power Systems*, vol. 38, no. 6, pp. 5701-5703, Nov. 2023.
  - [27] Y. Fang, S. Zhao, E. Du *et al.*, "Coordinated operation of concentrating solar power plant and wind farm for frequency regulation," *Journal of Modern Power Systems and Clean Energy*, vol. 9, no. 4, pp. 751-759, Jul. 2021.
  - [28] China Government Website. (2022, Mar.). Medium and long term plan for the development of hydrogen energy industry (2021-2035). [Online]. Available: [https://www.gov.cn/xinwen/2022-03/24/content\\_5680975.htm](https://www.gov.cn/xinwen/2022-03/24/content_5680975.htm)
  - [29] Y. Shu, L. Zhang, Y. Zhang *et al.*, "Carbon peak and carbon neutrality path for China's power industry," *Chinese Journal of Engineering Science*, vol. 23, no. 6, pp. 1-15, Jan. 2021.
  - [30] N. Shaukat, B. Khan, S. M. Ali *et al.*, "A survey on electric vehicle transportation within smart grid system," *Renewable and Sustainable Energy Reviews*, vol. 81, pp. 1329-1349, Jan. 2018.
  - [31] A. Arsalis, P. Papanastasiou, and G. E. Georghiou, "A comparative review of lithium-ion battery and regenerative hydrogen fuel cell technologies for integration with photovoltaic applications," *Renewable Energy*, vol. 191, pp. 943-960, May 2022.
  - [32] Z. Gu, G. Pan, H. Li *et al.*, "Provincial multistage power expansion planning toward coal and renewables positioning," in *Proceedings of 2023 IEEE International Conference on Energy Technologies for Future Grids (ETFG)*, Wollongong, Australia, Dec. 2023, pp. 1-6.
  - [33] Z. Gu, G. Pan, W. Gu *et al.*, "Assessment and prospect of region joint electrolytic hydrogen systems considering multiple energy sources: wind, solar, hydro and thermal power," *IEEE Transactions on Industry Applications*, vol. 59, no. 5, pp. 5269-5282, Sept. 2023.
  - [34] Global Energy Monitor. (2024, Jan.). Global coal plant tracker. [Online]. Available: <https://globalenergymonitor.org/projects/global-coal-plant-tracker/tracker/>
  - [35] Z. Gu. (2024, Feb.). Supplementary information of multistage provincial power expansion planning and market design toward energy transition: a case study of Xinjiang in China. [Online]. Available: <https://zenodo.org/records/10666221>
  - [36] M. Cuturi and M. Blondel, "Soft-DTW: a differentiable loss function for time-series," in *Proceedings of the 34th International Conference on Machine Learning*, Sydney, Australia, Apr. 2017, pp. 894-903.
  - [37] F. Petitjean, A. Ketterlin, and P. Gançarski, "A global averaging method for dynamic time warping, with applications to clustering," *Pattern Recognition*, vol. 44, no. 3, pp. 678-693, Mar. 2011.
  - [38] P. Bholowalia and A. Kumar, "EBK-means: a clustering technique based on elbow method and k-means in WSN," *International Journal of Computer Applications*, vol. 105, no. 9, pp. 1-8, Nov. 2014.
- Guangsheng Pan** received the B.S. and M.S. degrees in electrical engineering from Shandong University, Jinan, China, in 2014 and 2017, respectively, and the Ph.D. degree in electrical engineering from Southeast University, Nanjing, China, in 2022. He is currently an Assistant Research Fellow at the School of Electrical Engineering, Southeast University. His research interests include modeling, planning and optimization of integrated energy systems, and electrolytic hydrogen.
- Zhongfan Gu** received the B.S. degree in electrical engineering from Hohai University, Nanjing, China, in 2022. He is currently working toward the Ph.D. degree from the School of Electrical Engineering, Southeast University, Nanjing, China. His research interests include modeling, planning, and optimization of integrated energy systems.

**Yuanyuan Sun** received the B.S. and Ph.D. degrees in electrical engineering from the School of Electrical Engineering, Shandong University, Jinan, China, in 2003 and 2009, respectively. She is currently a Professor with the School of Electrical Engineering, Shandong University. Her current research interests include power quality of power system, flexible direct current system, and smart distribution network.

**Kaiqi Sun** received the B.S. and Ph.D. degrees in electrical engineering from Shandong University, Jinan, China, in 2015 and 2020, respectively. He was also a Visiting Scholar with the University of Tennessee, Knoxville, USA, from 2017 to 2020, and a Research Associate with the Department of Electrical Engineering and Computer Science, University of Tennessee from

2020 to 2021. He is currently an Associate Research Fellow with Shandong University. His research interests include DC system operation, renewable energy integration, and machine learning based power system application.

**Wei Gu** received the B.S. and Ph.D. degrees in electrical engineering from Southeast University, Nanjing, China, in 2001 and 2006, respectively. From 2009 to 2010, he was a Visiting Scholar in the Department of Electrical Engineering, Arizona State University, Phoenix, USA. He is now a Professor at the School of Electrical Engineering, Southeast University. He is the Director of the Institute of Distributed Generations and Active Distribution Networks, Nanjing, China. His research interests include distributed generation, microgrid, and integrated energy systems.